Coincident Radio Frequency and Optical Emissions from Lightning, Observed with the FORTE Satellite

T.E. Light, D.M. Suszcynsky, A.R. Jacobson

Space and Atmospheric Sciences Group, Los Alamos National Laboratory, Los Alamos, New Mexico

Short title: COINCIDENT RF/OPTICAL LIGHTNING EMISSIONS

Abstract. We present long optical and radio frequency (RF) timeseries of lightning events observed with the FORTE satellite in January 2000. Each record contains multiple RF and optical impulses. We identify the general type of discharge for each impulse using the discrimination techniques described by Suszcynsky et al. [2000], and reviewed herein. We see a large number of paired, impulsive events in the RF which allow us to study the heights within clouds of several events. We also see that the rate of RF/optical coincidence depends on the type of discharge: nearly 100% of VHF signals from first negative return strokes have an associated optical signal, whereas a mere 50% of impulsive intracloud events appear to have an optical counterpart. While the RF signals from ground strokes clearly coincide with simple optical signals in almost all cases, the intracloud lightning often shows nearly continuous, complicated RF and optical emissions which do not cleanly correlate with one another. The RF and optical pulses do not show a well-defined relationship of intensities, for any lightning type. The observed delay between the RF and optical pulses we interpret as mainly an effect of the scattering experienced by the light as it traverses the cloud. For intracloud lightning, we find no evidence of an intrinsic delay at the source between the onset of the RF and optical signals.

1. Introduction

Los Alamos and Sandia National Laboratories built the FORTE satellite and launched it in 1997. FORTE carries a suite of detectors that monitor lightning activity, and unlike previous lightning monitors, FORTE's instruments can record both the radio frequency (RF) and optical emissions from transient events in the Earth's atmosphere, on a routine, automated basis. Such a dual phenomenology approach to lightning detection results in a unique combination

of lightning and thunderstorm monitoring capabilities. Studying correlated optical and RF emissions from individual lightning events allows the RF signal to be used as a time fiducial, which facilitates estimation of the scattering delay of the optical light by intervening clouds.

The optical signals from lightning have been compared to lightning E-field changes a number of times. *Beasley et al.* [1983], for example, compared ΔE to light from stepped leaders, finding that pulses in each signal were simultaneous to within their measurement accuracy (± 0.2 μs) although not every ΔE pulse showed corresponding light. *Guo & Krider* [1982] studied return strokes, and found the light signal to begin at or just after the E-field peak, and also found that the optical peak is always greater for initial return strokes than for subsequent. *Ganesh et al.* [1984] similarly studied return strokes and saw a broad correlation between E-field intensity and light intensity. In this work we hope to see what general trends exist between VHF and optical lightning emission, as a function of lightning discharge type. Few previous studies have compared RF and optical lightning emissions. *Mazur et al.* [1995] compared high-speed video observations and those from a VHF interferometer, and saw temporal structure in the optical component of leader activity. *Suszcynsky et al.* [2000a] presented the first satellite-based comparison of optical lightcurves and RF power timeseries using data from the FORTE satellite. We now continue that work with a systematic comparison of VHF and optical emission as a function of lightning types.

2. The Data

2.1. The detectors

The FORTE Optical Lightning System (OLS) consists of two optical transient detectors. One is a fast, broadband photometer (the Photodiode Detector, or PDD), which records

time-series of events with 15 μs resolution (for greater detail, see *Kirkland et al.* [1998] or *Suszcynsky et al.* [2000a,b]). The PDD is sensitive from 0.4 to 1.1 μm, and records a lightcurve for events occurring within its 80° field-of-view ($\sim$ 1200 km footprint on the ground). (The OLS has a smaller field-of-view than the RF receivers, and therefore RF/optical coincident data is limited to events occurring within this footprint.) The second optical detector on FORTE is the Lightning Location System (LLS) – a 128-pixel by 128-pixel CCD array that can geo-locate events to within 10 km on the ground (see *Suszcynsky et al.* [2000b] for details). FORTE also carries three RF receivers, two of which are described elsewhere [*Jacobson et al.* (1999)]. Since January, 2000, FORTE data has been collected exclusively with the third, a broadband radio receiver with an analog bandwidth of 85 MHz and which digitizes at 300 Mega-samples per second (for a temporal resolution of 3.33 ns). It can trigger autonomously or it can be slaved to trigger only when the LLS triggers. In the slaved configuration, whenever the LLS detects an event, both the PDD and the RF trigger, and the 8.7 ms (RF) or 6.85 ms (PDD) of data preceding the trigger are recorded as the event. In this present work, we consider the slaved PDD data and the low-band, slaved, RF data. In this frequency range, the RF data is heavily contaminated by anthropogenic carrier signals, however, so that we restrict ourselves to data in the 29-49 MHz subband in the RF.

2.2. Data selection

Because all the data in this present study were collected with the optical and RF detectors in slave-mode, we are guaranteed to have a geolocation for every data record. However, the LLS is sensitive to glint (e.g., off of the satellite or off of water), cloud albedo, and energetic particles. We therefore found all the slaved data archived from January 2000 and rejected

first any non-lightning LLS events. We next rejected daytime events, as the FORTE optical nighttime data are higher quality than daytime data. (We can set the triggering thresholds lower for nighttime data collection, and therefore the nighttime data set is less biased towards very bright events, as well as being less subject to trigger on glint or cloud albedo.) Finally we rejected any event where the RF was contaminated by radar signals.

We were left with 222 high quality, RF/optical coincident records. Often, several records occur sequentially, within a few hundred milliseconds. Figure 1 shows the distribution of inter-record times for all the sequentially recorded RF-optical coincident records whose LLS geolocations indicate they are less than 50 km apart, from data taken between January and April of 2000. It appears that records further than $\sim$ 500 ms apart are not associated with one another, whereas more tightly spaced records can be grouped into flashes. Thus, spatially co-located data records which are spaced in time by less than 500 ms we assume to be subsequent triggers from a single flash.

Figure 2 illustrates a data set for a single flash, in which we obtained five records within 86 ms. However, FORTE cannot retrigger instantaneously, but rather there is a delay after each record at least equal to an individual record length. Therefore our flash-length data sets are actually made up of snapshots within the flash. For example, in plate 1 it is clear how these five events, while seen sequentially by the satellite, do not offer a complete picture of the flash.

2.3. Data Processing

These FORTE/RF power timeseries have 2,621,440 points with $\sim$ 3 ns resolution, spanning $\sim$ 8 ms. We bin this data to 1 μs resolution to create a more manageable data file,

in which we can study correlations of RF events with individual optical pulses, as a function of RF event type. First, however, each record must be processed and individual discharges identified.

Each record is examined in turn. We first prewhiten and dechirp the RF spectrogram, as described in detail by *Jacobson et al.* [1999] to remove anthropogenic RF carrier bands and the frequency-dependent ionospheric dispersion of the RF signal. The resulting "clean" spectrogram is then averaged over frequency, returning a simple RF power timeseries for the event. The optical data is recorded as a simple timeseries of optical irradiance, and is therefore used in its original state.

Suszcynsky et al. [2000b] describe a technique to discriminate intracloud from cloud-to-ground discharges in FORTE/RF data. This procedure was created specifically with reference to the shorter (800 μs) RF records collected by FORTE. Each of the longer records studied in this present work, however, generally include multiple discharge events. We therefore could identify several individual events within each long record; within these 222 records, we identified a total of 647 individual events. Briefly, we differentiate various lightning events based on the RF power timeseries as follows. See figure 3 for an example of each type.

Cloud-to-ground activity

Initial negative return stroke: steady increase of RF signal over 1 ms or more (leader activity), with a sharp increase at the time of attachment, and a fairly quick recovery to background levels.

Subsequent negative return stroke: Wide events (up to 500μs) with a very sharp falloff.

Initial positive return stroke: Wide events (up to 500μs) with a very sharp

onset. (No leader activity.)

In-cloud activity

Impulsive events: Narrow events (less than 50μs) which rise to several times the background level (Signal-to-noise $\geq 5 \rightarrow 10$.)

Non-impulsive events: General, in-cloud events; broad (up to 500μs), with a slow rise and slow fall.

Mixed events: Events which show a non-impulsive event underlying one or more impulses.

We use the term "non-impulsive (NI) event" loosely in this context, meaning a temporally diffuse, in-cloud event. These events do not show the sharp onset or cutoff typical of a ground stroke, as found by examining the NLDN coincidence with FORTE/RF data [*Suszcynsky et al.* 2000b]. We speculate that this class of events must include a number of phenomena, such as the E-field K-changes described, for example, by *Uman* [1987]. We note, however, that K-changes typically are spaced in time by a few to several milliseconds, whereas in this data we often see NI events spaced by only hundreds of microseconds, or less.

The optical pulses also must be individually measured. Often an optical record includes several optical signals, blended to create a broad, multi-peaked lightcurve. As a result, we cannot measure the width of individual curves down at the 20%-of-peak level. Thus, in order to get some idea of the rise time and width of individual optical pulses, we fit a parabola to each peak and calculate rise times and widths on the basis of these fits. Widths estimated in this way are not truly representative of the pulse width, since the parabolic fit will neglect the long tail of the optical pulses. However, this allows us an internally consistent measure optical

pulse parameters.

3. Comparing RF and optical pulses

While identifying individual RF events and individual optical pulses, we also paired them on the subjective basis of whether the optical pulses appeared to coincide with the RF. For example, let us reconsider figure 2. In the earliest record, there appear to be two RF and two optical pulses, although the second RF event is so broad and weak, it is not measurable. The next three records again shows a pulse-for-pulse coincidence. In the fourth record, however, the RF "pulse" associated with the optical signal is in fact several impulses occurring over ~ 600 μs. The final record shows two distinctly separate, weak pulse-pairs in the RF and a broad, weak optical signal. Which pulse pair, if either, is directly associated with the optical signal is unclear, and therefore we measure the RF and optical events, without assigning them as a matched RF/optical set.

The disadvantages of our procedure are obvious. First, it is subjective and phenomenological. Second, we are biased to labeling as pairs those events in which the RF signal precedes the optical, because the optical light is scattered and delayed as it traverses the cloud, and therefore even if it were emitted exactly coincidently with the RF, it would be observed as delayed. Finally, the lack of a counterpart for any RF or optical event in our database does not absolutely mean that there was no such counterpart; merely that it could not be identified clearly enough.

We therefore offer the following caveat to our RF/optical correlations. The RF/optical coincidence for ground strokes was quite clear; typically, for ground strokes, neither the RF nor optical signals were cluttered, and both were strong. For impulsive, in-cloud events, however,

the RF/optical correspondence was seldom clear; hence we probably have some number of pairings in the database which are loosely related at best.

3.1. General statistics

Table 1 lists some statistics, grouped by event type. 647 individual events were measured in the 222 files; 217 were RF signals without an optical counterpart, 128 were optical signals without an RF counterpart, and 302 were events for which both an optical and RF signal was present and measurable. Of the 45 initial negative return strokes identified, 100% showed optical counterparts. For ground strokes in general, $\sim 84\%$ have optical counterparts. Compare this to $\sim 52\%$ for in-cloud lightning. Furthermore, the in-cloud lightning is more likely to be contaminated with random, apparent RF/optical coincidences, due to the diffuse, quasi-continuous nature of the in-cloud, RF emissions, and the consequent difficulties in associating a string of RF impulses with an optical pulse. Thus, $\sim 52\%$ must be considered an *upper limit* to the RF/optical coincidence rate of IC lightning.

Table 1

It may be wondered whether the slight difference shown among types in Table 1 for the peak RF power – it is slightly higher for 1st -RS – is responsible for the differentiated incidence of optical counterparts. Yet figure 4 shows that regardless of peak power, it is mainly the type of RF event and not the RF intensity that determines the optical coincidence rate.

3.2. RF versus Optical Power

There is no detailed correspondence between the RF and optical pulse peak intensities in the data. This is presumably due in part to the considerable variability of optical scattering losses across a range of cloud types; depending on the event's placement in a cloud, the cloud optical depth, and the observer's viewing angle, the same event could be attenuated in

observed peak amplitude by up to 2-3 orders of magnitude [*Light et al.* 2000]. In figure 5 we see that the observed RF and optical peaks do broadly correlate, but with considerable spread. Here again we see a slight differentiation by event type, with ground strokes somewhat stronger in both types of emission.

3.3. Effects of Optical Scattering

We use the peak of the RF signature from the lightning as a time fiducial in order to estimate the delay of the optical signal due to scattering by clouds. For the case of return strokes, we might assume that there is an additional delay between the RF and the optical emission which is the time necessary for current to propagate up the channel, after the return stroke attachment, back into the cloud, from whence the optical emission is detected; this delay is presumed to be on the order of $50 - 100$ μs. (See for example, *Ganesh et al.* [1984] and references therein.) Thus we can estimate the contribution to the observed RF-optical delay which is due to scattering [*Suszcynsky et al* 2000a]:

$$\Delta t_{rf-opt} = \Delta t_{physical} + \Delta t_{scatter}$$

In the case of intracloud emission, however, it is unclear what to expect for the value of $\Delta t_{physical}$.

We wish to measure the "lag", $\Delta t_{physical}$, for IC and CG lightning which we define as the time from the RF peak to the onset of the optical signal. Optical onset we determine by subtracting the rise time (which includes the delay due to scattering) from the optical time of peak. This results in a distribution of lags which ranges from -2 ms to +1.3 ms. The largest lags, either positive or negative, must be the result of incorrectly-paired RF and optical signals. We therefore perform a sigma-clipping of the 302 RF/optical coincident events, dropping from

the database seven events for which the lag is more than 3σ from the mean lag of the entire population. In fig. 6 we plot histograms of the remaining lags and mark the the mean and standard deviation, for ground strokes and in-cloud events. We know that $\Delta t_{scatter} \geq 0$. The data is therefore consistent with there being a physical delay between the RF peak and the optical signal onset of $\Delta t_{physical} \simeq 60$ μs for ground strokes and $\Delta t_{physical} \simeq -33$ μs for IC lightning. This value for the ground strokes is consistent with previous estimates [*Suszcynsky et al.* 2000a; *Ganesh et al.* 1984]. This is also consistent with the finding of *Jacobson et al.* [2000], that ground strokes tend to be observed by FORTE up to ~ 50 μs after being detected by the NLDN (see that paper's figure 3). For the cloud discharges, *negative* lags suggest that the optical signal onset often precedes the RF peak. In fig. 7 we show some examples; these records are typical of those in which several cloud events occur in succession, and show clearly that the optical light pulses begin before the RF peaks, and indeed some begin nearly simultaneously with their corresponding RF event; thus the optical light must have been emitted earlier than or coincident with the RF emission.

This result has implications for the temporal relationship of the RF emission and current flow. We assume that to within the resolution of our measurements, the optical emission and current flow are simultaneous [*Beasley et al.* 1983; *Gomes & Cooray* 1998]. Therefore we consider the optical emission onset as a proxy for the onset of current flow, and let the RF indicate the time rate of change of the current. Thus in the case of return strokes, there is a strong, abrupt, brief current coincident with the attachment, creating a brief optical signal which is then delayed and broadened by passage through the cloud and observed after the sharp RF signal. IC lightning on the other hand, must involve a considerably more gradual current increase, creating broad optical and RF waveforms, and despite scattering, the optical

light begins escaping before the RF has peaked.

3.4. General Observations

Several features in these waveforms become apparent as one sifts through hundreds of examples, which are difficult to quantify statistically, but which could be called "commonly seen". Below we briefly describe a few of these observations.

- For initial, negative return strokes, we often see low-level light preceding the main optical pulse, corresponding to the optical counterpart of the leader activity. (See fig. 8(a,b) for an example.) Also, we sometimes see structure in the optical leader, in which the light waxes near the leader onset, wanes, and then reasserts just before the return stroke. A similar pattern was seen in at least one return stroke leader observed by *Mazur et al.* [1995].

  In fig. 8(a) there is the suggestion of discrete leader steps, approximately 4 ms before the attachment, which gradually blur into continuous leader emission. This is *not* a commonly seen feature, perhaps because we do not often have several milliseconds of leader activity recorded for a return stroke.

- Initial negative return strokes are very commonly followed immediately (within 50-300 μs) by some form of cloud discharge, usually a doublet of NI events (fig. 8(b)).

- We saw two cases (4%) where the optical counterpart to a 1st -RS is double-peaked, with the optical peaks spaced by $\sim$ 700 μs. We note that *Guo & Krider* [1982] similarly saw that the optical signals from $\sim$ 5% of first return strokes had a second peak, but with no corresponding second peak in the E-field signature. Those authors assume these

secondary peaks to be caused by branches or M-components.

- The RF pulses of IC activity tend to occur in the context of extended, multi-peaked optical emission, rather than to be associated with specific peaks of light (fig. 8(c,d)).

4. RF Pulse Pairs

In the self-triggered FORTE/RF data, so-called "transionospheric pulse pairs" (see *Holden et al.* [1995]) are among the strongest events seen, and we see few ground strokes. These pulse pairs are a VHF pulse and its reflection off the ground, each seen by the satellite after traversing slightly different paths and therefore the secondary (reflection) is delayed by an amount proportional to the event's height off the ground [*Massey & Holden* (1995), *Massey et al.* (1998)]. The event height can be calculated if one knows the latitude and longitude of the event and the position of the satellite. These present data are triggered by the OLS and in them we see a high incidence of weak pulse pairs that would not have triggered the RF receiver on their own, while the most powerful events we see are initial, negative return strokes. This reinforces the impression that impulsive, in-cloud discharges in general are not associated with strong optical counterparts. Extended IC emission, however, typically includes several weak impulsive events and enough light to trigger the optical sensors. We therefore have a sample of pulse pairs unbiased by peak RF pulse power with which we can explore *i)* the rate of occurrence of impulsive RF events, and *ii)* the vertical distribution of lightning within each record or within each flash or storm using the event heights derived from the the inter-pulse times. (Because all the data in this study are geolocated with the FORTE/LLS, each pulse pair provides an event height estimate.)

To build a database of impulse parameters, we identify pulse pairs manually within each

record, selecting the peaks of the primary and reflected pulse, and then in software calculate the event height for each primary impulse. This procedure is straightforward for isolated pairs, but occasionally there are sequences of multiple impulses which complicate matters. We interpret these as pair multiplets, and accordingly we group them into pairs whenever possible. Sometimes it is not possible to do so. For example, if only an odd number of impulses are obvious (e.g., due to poor signal-to-noise), it becomes unclear which may be paired. Such cases are left out of the database.

There were, on average, 7 impulse pairs found per flash, with an average rate of 1.2/ms, once they start occurring. (Often, the first few records in a flash will not have any impulses, and then there are several records containing IC impulses. We calculated the rate from the time of the initial pulse pair to the final one.) Table 2 lists some statistics for the 290 pulse pairs measured. The height shown is the event height, in kilometers, calculated using the LLS geolocation. We define the "ratio" to be the ratio of the peak power of the primary (first) impulse to that of the reflected impulse.

Table 2

The peak of the primary impulse does not vary as a function of the event height, nor as a function of when the impulse occurs during the flash. The height-spread within a single flash is typically less than a kilometer, but can range up to about 6 km (fig. 9). We looked at whether we could detect the bi-level structure in individual IC flashes [e.g., *Shao & Krehbiel* 1996; *Thomas et al.* 2000], but with only a few pulse pairs within any given flash with which to probe the event heights, this structure was not obvious.

Figure 9 also shows the overall distribution of event heights. The distribution is fairly constant from 6-13 km, but then falls off sharply with fewer than 10 events at 13-16 km. *Smith et al.* [1999] show the height distributions of narrow negative and positive bipolar events as

measured with the Los Alamos Sferic Array. The distribution in fig. 9 is consistent with that of their narrow positive bipolar events, but their distribution of negative events is at markedly higher altitudes ($\sim$ 15-20 km).

5. Summary

We compared individual RF and optical pulses from lightning observed with the FORTE satellite. More than 80% of ground strokes showed obvious, associated optical and RF signals; only $\sim$ 50% of in-cloud events showed similar RF/optical correspondence. The peak RF and optical power in related pairs of pulses correlate over several orders of magnitude, although the relation is broad, due presumably to losses of the optical light by scattering in clouds. Ground strokes are among the strongest events seen, in both optical light and RF, while impulsive, in-cloud events are among the weakest.

Using the RF discharge as the time fiducial, we find that for ground strokes there appears to be a small delay between emission of the RF and optical signals, $\langle \Delta t_{CG} \rangle = 59$ μs. For in-cloud events, however, the optical signal onset often precedes the peak of the RF, $\langle \Delta t_{IC} \rangle = -33$ μs. This implies that the optical light must have been emitted earlier than or coincident with the onset of the RF signal.

Optical light from leader activity was commonly seen, and rather than monotonically increasing like the RF leader, the optical leader often decreases mid-way through, and increases again near the time of the return stroke. While the RF and optical light from return strokes typically appear as strong and unambiguous bursts, the RF pulses of IC activity tend to occur within the context of extended, multi-peaked optical emission.

Using RF pulse-pairs due to reflection of a pulse off the ground, we estimate the heights

of several in-cloud events. The height distribution ranges from 6-13 km, and falls off sharply at higher altitudes.

Acknowledgments. The authors would like to thank the entire FORTE Science and Operations team at Los Alamos and Sandia National Laboratories for useful discussions regarding the FORTE sensors and data, and in particular Jose Guillen and Jeff Green of Sandia for their insights into the optical detectors. This work was supported by the U.S. Department of Energy.

References

Beasley, W.H., M.A. Uman, D.M. Jordan & C. Ganesh, Simultaneous Pulses in Light and Electric Field from Stepped Leaders Near Ground Level, *Jour. Geophys. Res. - Atmos., 88,* 8617-8619, 1993.

Ganesh, C., M.A. Uman, W.H. Beasley & D.M. Jordan, Correlated Optical and Electric Field Signals Produced by Lightning Return Strokes, *Jour. Geophys. Res. - Atmos., 89,* 4905-4909, 1984.

Gomes, C. & V. Cooray, Correlation Between the Optical Signatures and Current Wave Forms of Long Sparks: Applications in Lightning Research, *Jour. of Electrostatics, 43,* 267-274, 1998.

Guo, C. & E.P. Krider, The Optical and Radiation Field Signatures Produced by Lightning Return Strokes, *Jour. Geophys. Res. - Atmos., 87,* 8913- 8922, 1982.

Holden, D.N., C.P. Munson & J.C. Devenport, Satellite Observations of Transionospheric Pulse Pairs, *Geophys. Res. Lett., 22*(8),889-892, 1995.

Jacobson, A.R., S.O. Knox, R. Franz & D.C. Enemark, FORTE Observations of Lightning Radio-Frequency Signatures: Capabilities and Basic Results, *Radio Sci., 34*(2), 337-354, 1999.

Jacobson, A.R., K.L. Cummins, M. Carter, P. Klingner, D. Roussel-Dupré & S.O. Knox, FORTE Radio-Frequency Observations of Lightning Strokes Detected by the National Lightning Detection Network, *Jour. Geophys. Res. - Atmos., 105,* 15,653-15,662, 2000.

Kirkland, M.W., D.M. Suszcynsky, R.C. Franz, J.L.L. Guillen & J.L. Green, Observations of Terrestrial Lightning at Optical Wavelengths by the Photodiode Detector on the FORTE Satellite, *Tech. Rep. LA-UR-98-4098*, 14 pp., Los Alamos Natl. Lab, Los Alamos, NM, 1998.

Light, T.E., D.M. Suszcynsky & A.R. Jacobson, Simulations of Lightning Optical Waveforms as Seen Through Clouds by Satellites, *submitted to Jour. Geophys. Res - Atmos.,* 2000.

Massey, R.S. & D.N. Holden, Phenomenology of Transionospheric Pulse Pairs, *Radio Sci., 30*(5), 1645-1659, 1995.

Massey, R.S., D.N. Holden & X.-M. Shao, Phenomenology of Transionospheric Pulse Pairs: Further Observations, *Radio Sci., 33*(6), 1755-1761, 1998.

Mazur, V., P.R. Krehbiel & X.-M. Shao, Correlated High-Speed Video and Radio Interferometric

Observations of a Cloud-to-Ground Lightning Flash, *Jour. Geophys. Res. - Atmos., 100,* 25,731-25,753, 1995.

Shao, X.-M. & P.R. Krehbiel, The Spatial and Temporal Development of Intracloud Lightning, *Jour. Geophys. Res. - Atmos., 101,* 26,641-26,668, 1996.

Smith, D. A., J. Harlin, X. M. Shao, K. B. Eack, Lightning Location, Classification, and Parameterization with the Los Alamos Sferic Array, EOS Trans. AGU, 80(46), Fall Meet. Suppl., F203, 1999.

Suszcynsky, D.M., M.W. Kirkland, A.R. Jacobson, R.C. Franz, S.O. Knox, J.L.L. Guillen & J.L. Green, FORTE Observations of Simultaneous VHF and Optical Emissions from Lightning: Basic Phenomenology, *Jour. Geophys. Res. - Atmos., 105,* 2191-2201, 2000a.

Suszcynsky, D.M., T.E. Light, S.M. Davis, J.L. Green, J.L.L. Guillen, & W. Myre, Coordinated Observations of Optical Lightning from Space Using the FORTE Photodiode Detector and CCD Imager, *submitted to Jour. Geophys. Res - Atmos.,* 2000b.

Thomas, R.J., P.R. Krehbiel, W. Rison, T. Hamlin, J. Harlin, & D. Shown, VHF Source Powers Radiated by Lightning Discharges, *submitted to Geophys. Res. Lett.,* 2000.

Uman, M.A., *The Lightning Discharge*, Academic Press, Orlando, Florida, 1987.

A. R. Jacobson, T. E. Light, and D. M. Suszcynsky, Space and Atmospheric Sciences Group, NIS-1, Mail Stop D466, Los Alamos National Laboratory, Los Alamos, NM, 87545. (e-mail: tlavezzi@lanl.gov; dsuszcynsky@lanl.gov; ajacobson@lanl.gov)

Received _____

Figure 1. Distribution of time between sequentially-recorded, spatially co-located records. The smaller plot is a linearly-scaled blow-up of the peak in the larger, logarithmic plot. The inter-record time appears to rise above the random background for spacings less than $\sim$ 500ms.

Figure 2. An example of coincident RF/optical data from FORTE for a flash in which the detectors triggered five times within 86 ms; the vertical units are arbitrary as the records have been normalized in order to show the optical and RF intensity of each feature relative to the brightest features in the flash group. The RF and optical data have 2μs and 15μs resolution, respectively.

Figure 3. Examples of each type of event identified with our discrimination techniques.

Figure 4. The percentage of RF events that have optical counterparts, as a function of RF event type and RF peak power (actually the square of the E-field, $E^2 \sim V^2/m^2$).

Figure 5. Optical peak irradiance versus RF peak power ($E^2 \sim V^2/m^2$), differentiated by event type. Dots indicate ground strokes, triangles indicate impulsive cloud events, and asterisks indicate non-impulsive cloud events.

Figure 6. Histograms of the RF-optical lag for **(a)** IC and **(b)** CG events. The mean of each distribution is marked, and the horizontal error bar indicates the standard deviation on the mean.

Figure 7. A few typical RF and optical coincident waveform sets, showing intracloud lightning. These are not full 8 ms records; we have excerpted sub-records for clarity. The RF and optical light have been normalized by the peak emission in each record, to allow direct comparison in a single plot. The RF has been binned to 5 μs resolution.

Figure 8. Examples of commonly-seen features in the database, as described in the text. The optical and RF curves have 15 μs and 5 μs resolution, respectively.

Figure 9. **(a)** The range of heights measured for RF pulse pairs which occur in the same flash. **(b)** The overall distribution of heights measured for all 290 pulse pairs.

Plate 1. The RF power and optical irradiance versus time, for the data in fig. 2, presented on a single, compressed timescale in order to show when the five events occurred relative to one another over the span of 86 ms.

Table 1. General statistics of individually measured pulses

Event Type	N_{RF}	$N_{with\ opt.}$	RF peak $(mV/m)^2$	Opt. peak $(\mu W/m^2)$
			mean (median) ± std. dev	
CG EVENTS				
1st -RS	45	45	0.73 (0.40) ± 1.1	1066 (487) ± 1097
Subseq. -RS	16	11	0.71 (0.13) ± 1.8	77 (57) ± 56
1st +RS	35	25	0.39 (0.11) ± 0.79	304 (176) ± 503
IC EVENTS				
Impulsive	216	81	0.12 (0.054) ± 0.25	84 (49) ± 95
Non-impulsive	173	113	0.20 (0.070) ± 0.37	239 (116) ± 423
Mixed	33	27	0.082 (0.055) ± 0.083	132 (83) ± 143
UNTYPED – optical only				
	0	128	···	161 (57) ± 437

Table 2. General statistics of 290 RF pulse pairs

	Height (km)	Ratio of peaks	RF peak (mV^2/m^2)	Rate (pairs/ms)	Number per flash
Mean	10.12	1.32	0.081	1.15	7
Std. Dev.	2.2	0.95	0.20	1.53	6
Median	10.20	1.12	0.031	0.70	5
Minimum	6.10	0.04	0.0017	0.02	1
Maximum	15.50	10.8	2.1	5.98	34

Figure 1

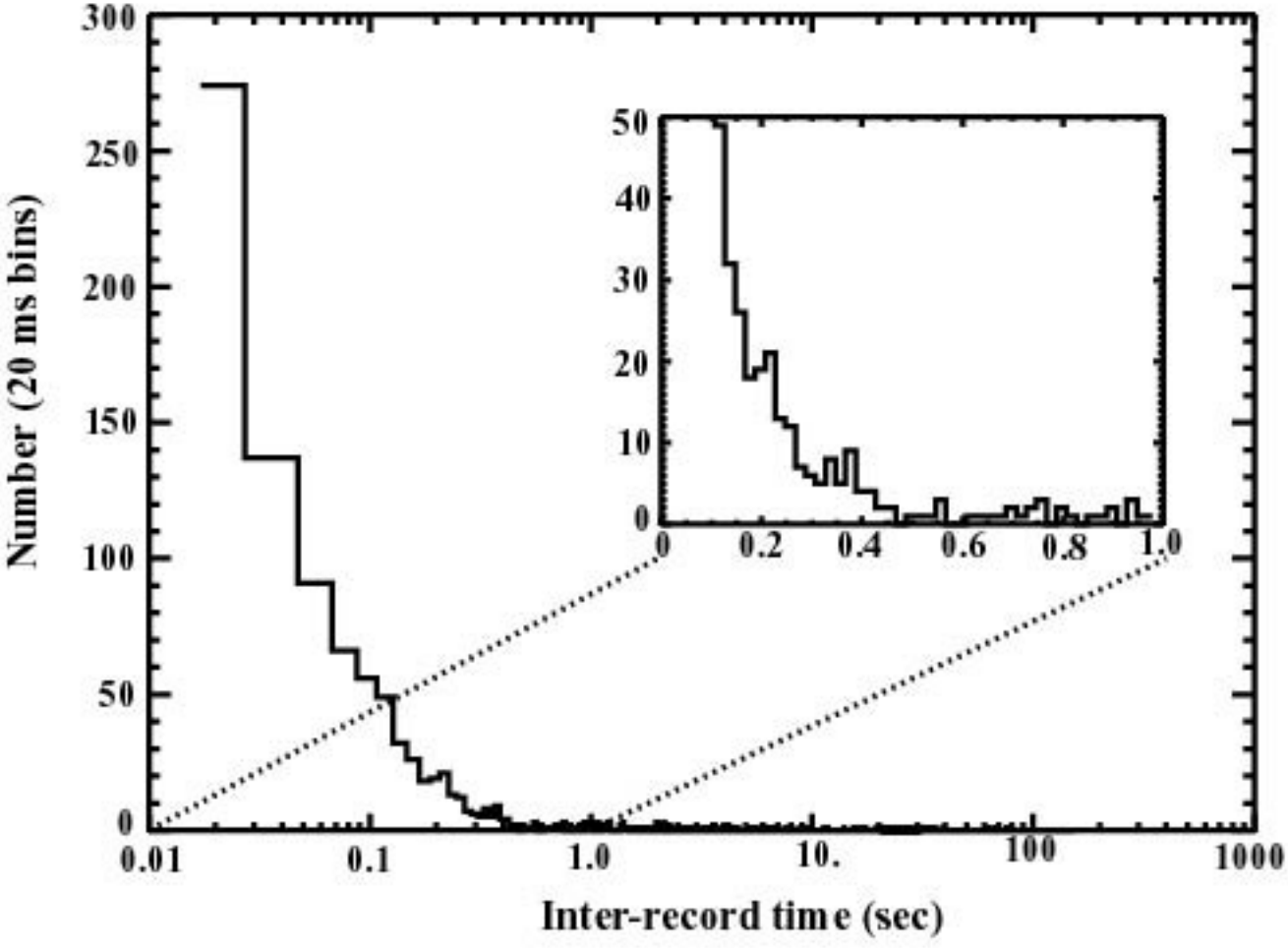
Number (20 ms bins)
300
250
200
150
100
50
0
0.01
0.1
1.0
10.
100
1000
Inter-record time (sec)
50
40
30
20
10
0
0
0.2
0.4
0.6
0.8
1.0

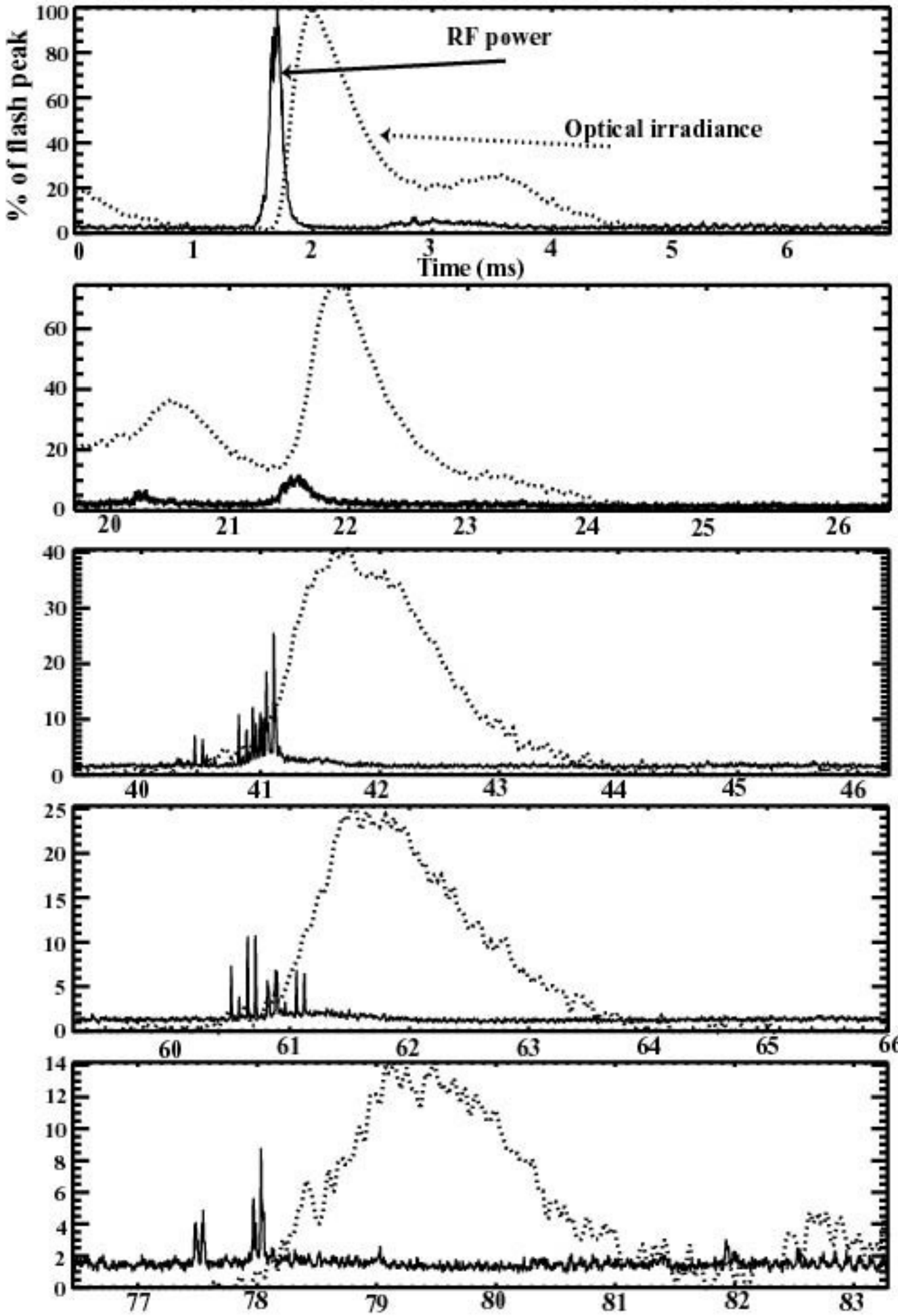

Figure 2

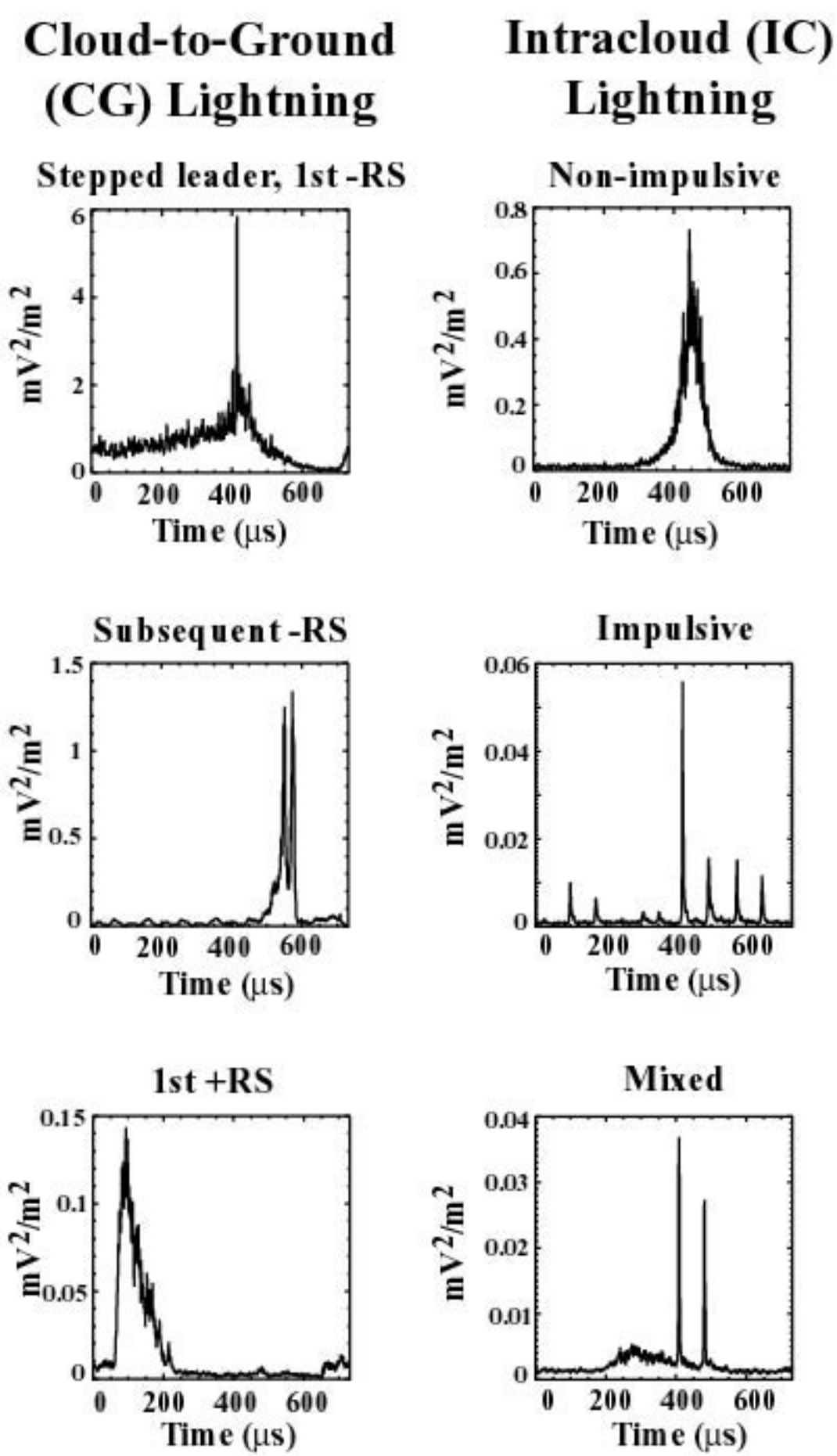
Cloud-to-Ground (CG) Lightning
Intracloud (IC) Lightning
Stepped leader, 1st -RS
Non-impulsive
Subsequent -RS
Impulsive
1st +RS
Mixed
mV2/m2
Time (μs)
0
200
400
600
6
4
2
0.8
0.6
0.4
0.2
1.5
1
0.5
0.06
0.04
0.02
0.15
0.1
0.05
0.03
0.01

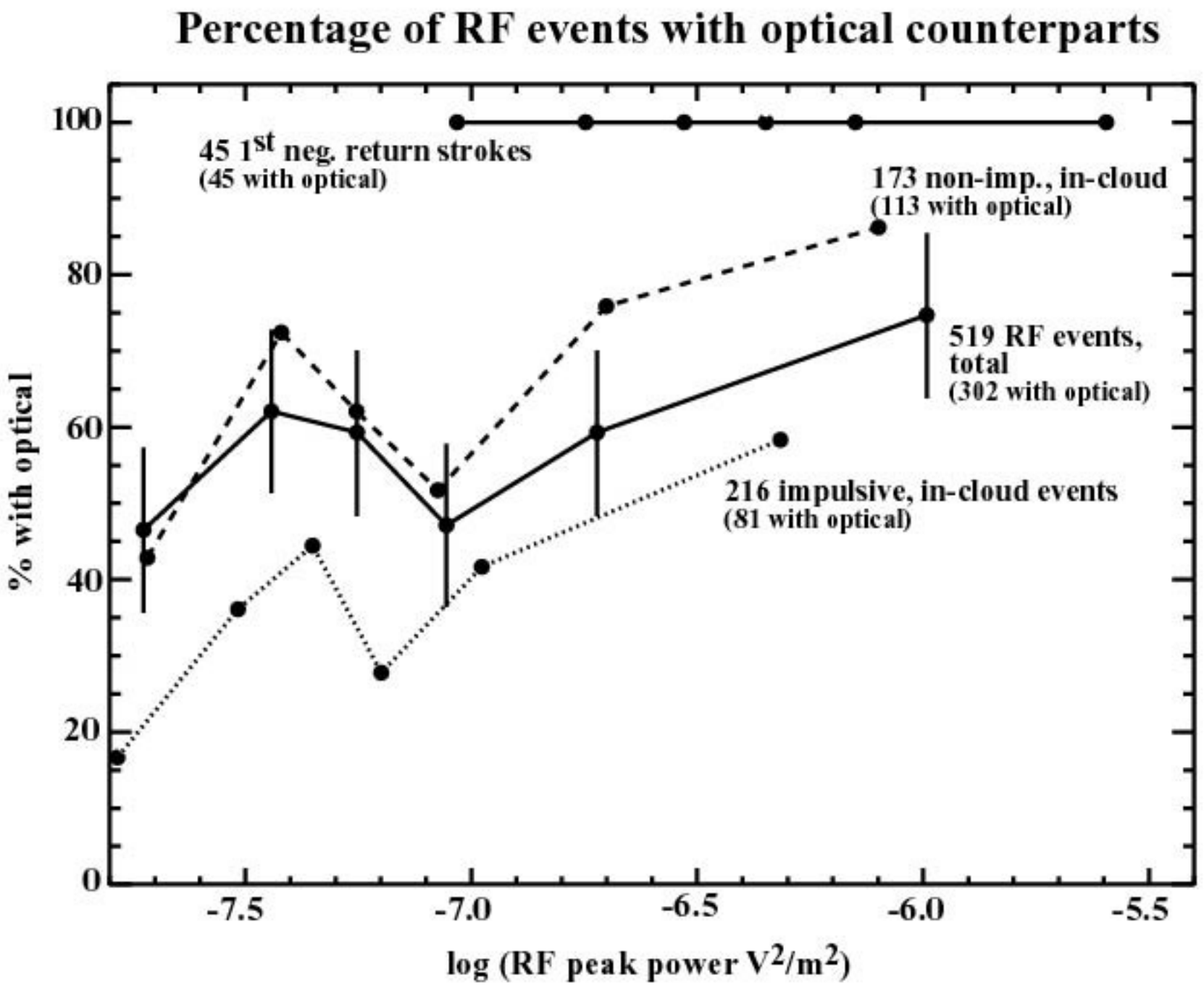
Percentage of RF events with optical counterparts
45 1st neg. return strokes
(45 with optical)
173 non-imp., in-cloud
(113 with optical)
519 RF events,
total
(302 with optical)
216 impulsive, in-cloud events
(81 with optical)
% with optical
100
80
60
40
20
0
-7.5
-7.0
-6.5
-6.0
-5.5
log (RF peak power V2/m2)

Figure 4

Figure 5

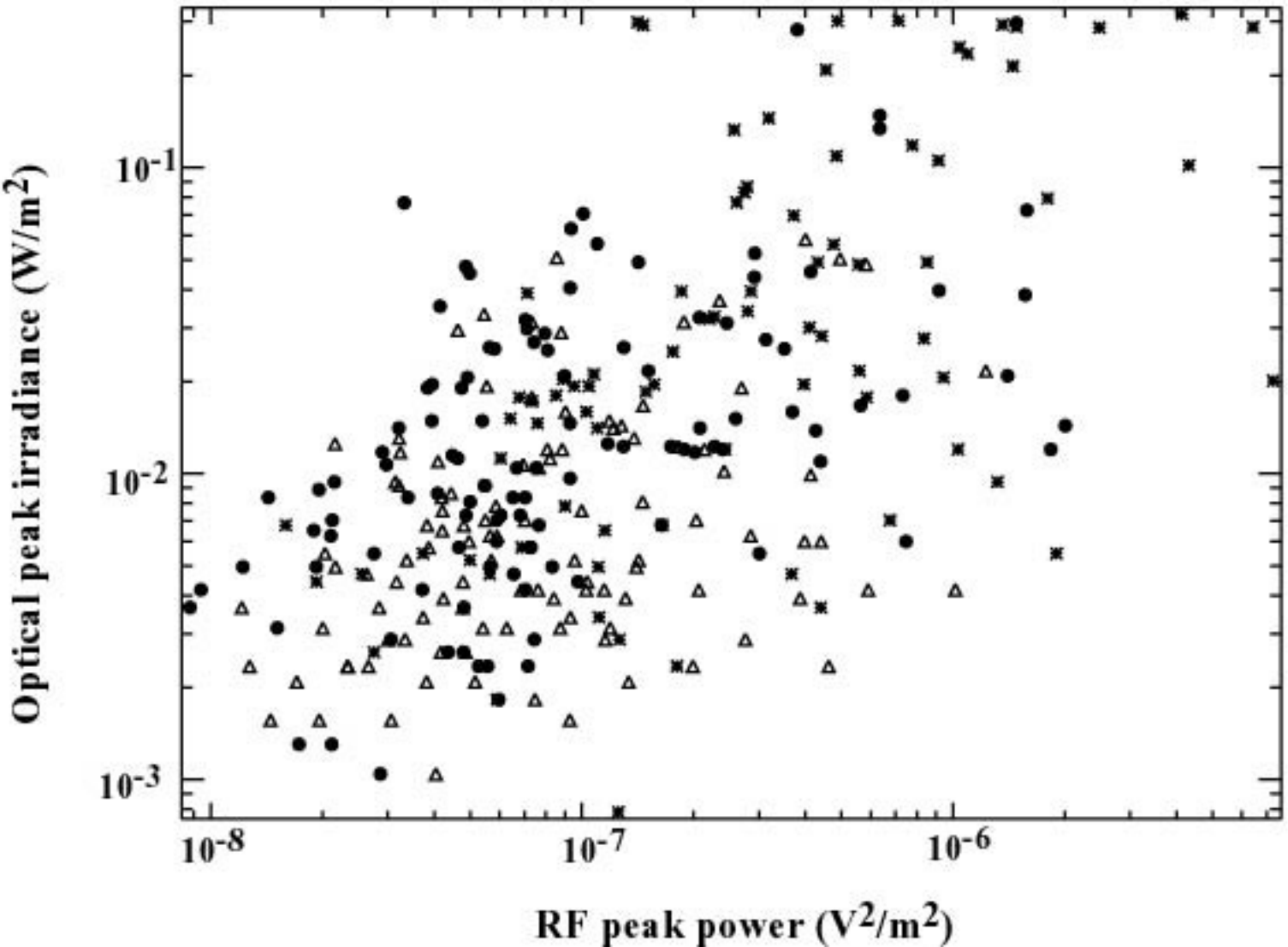
Optical peak irradiance (W/m²)
10⁻¹
10⁻²
10⁻³
10⁻⁸
10⁻⁷
10⁻⁶
RF peak power (V²/m²)

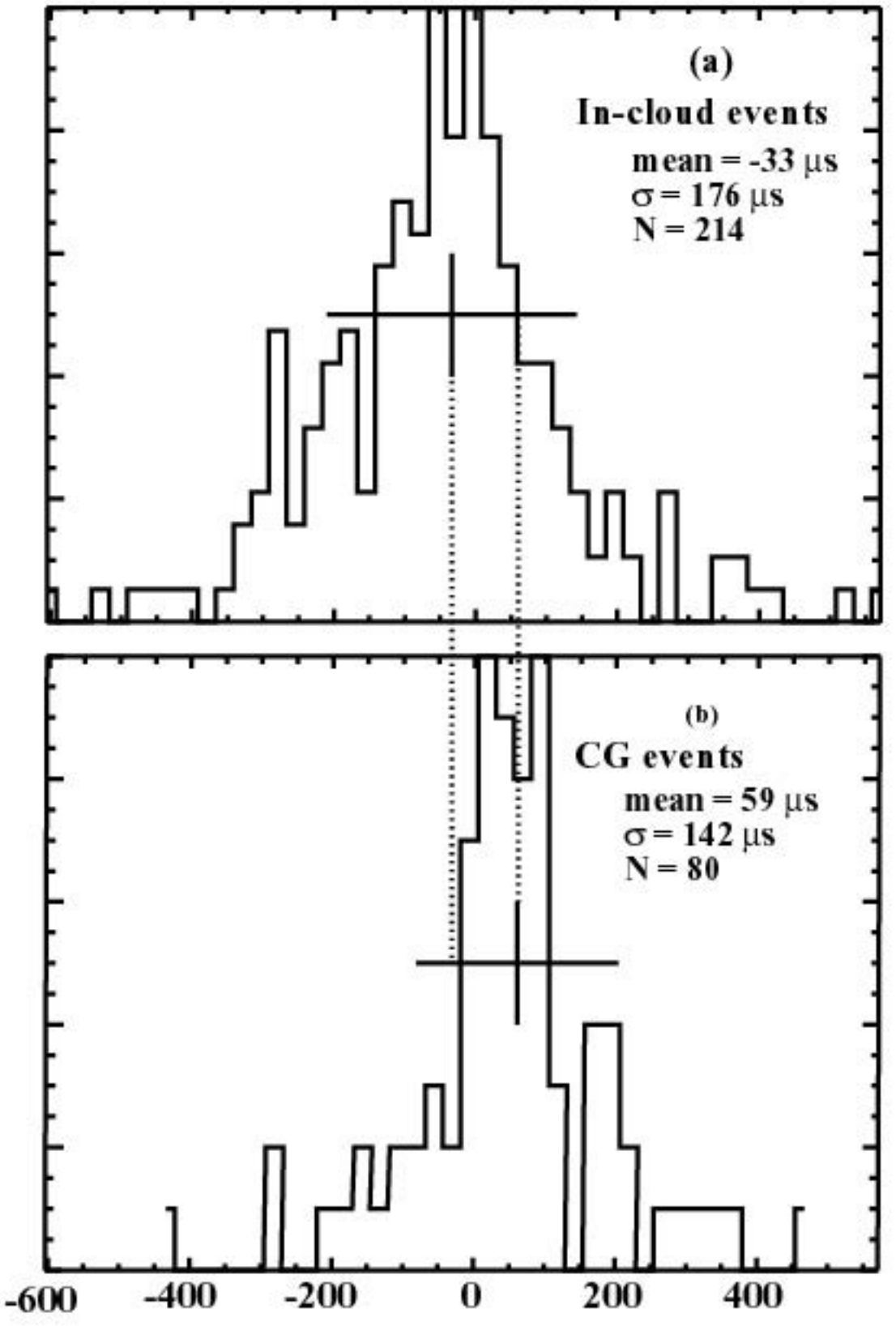
(a)
In-cloud events
mean = -33 μs
σ = 176 μs
N = 214
(b)
CG events
mean = 59 μs
σ = 142 μs
N = 80
-600
-400
-200
0
200
400
Distribution of Optical-RF lag times (μs)

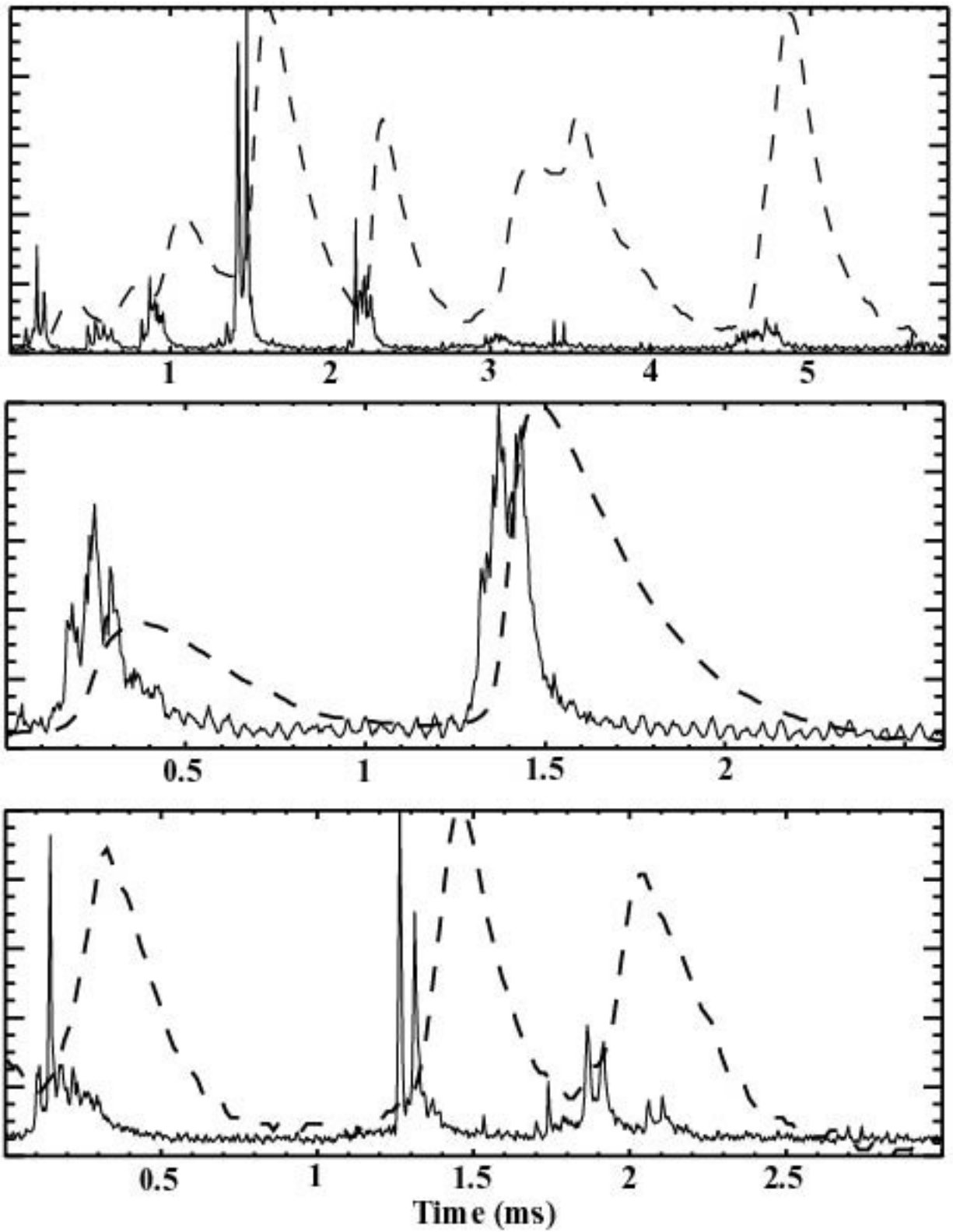
1
2
3
4
5
0.5
1
1.5
2
0.5
1
1.5
2
2.5
Time (ms)

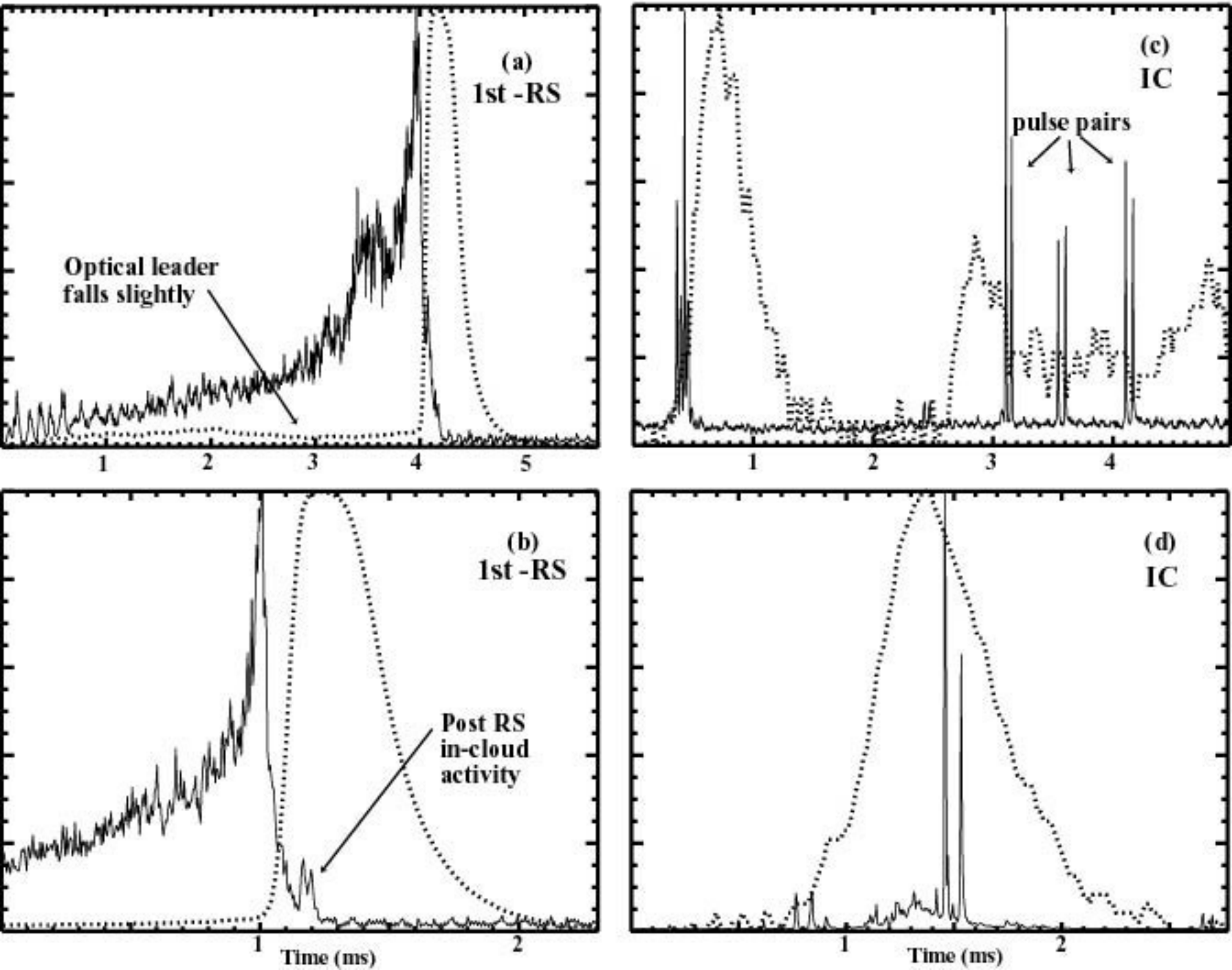
(a)
1st -RS
Optical leader
falls slightly
1
2
3
4
5
(c)
IC
pulse pairs
1
2
3
4
(b)
1st -RS
Post RS
in-cloud
activity
1
2
Time (ms)
(d)
IC
1
2
Time (ms)

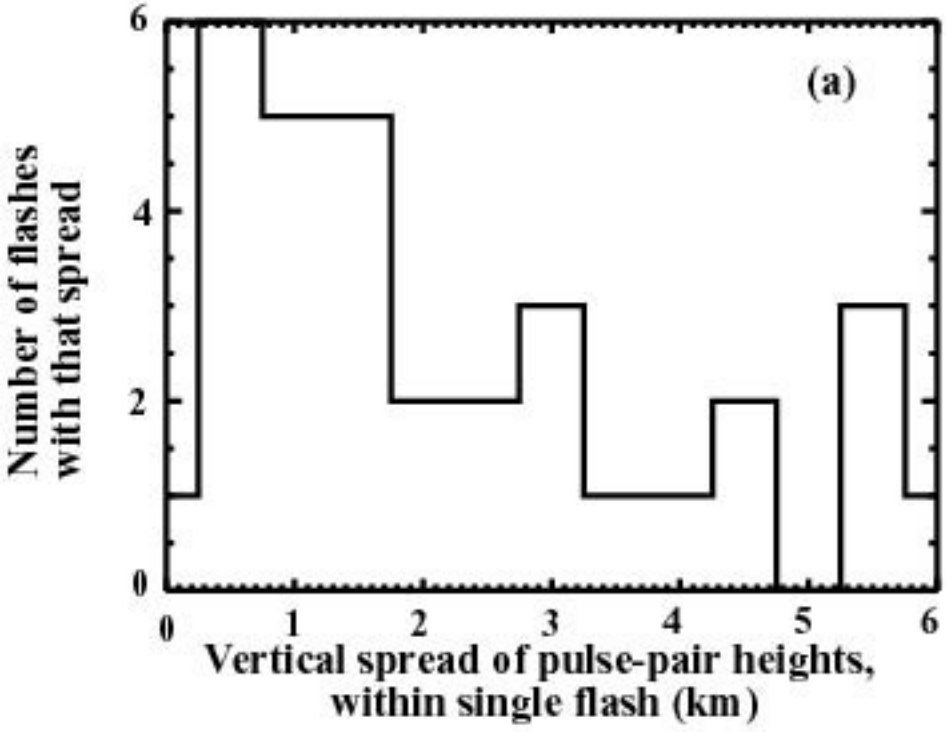
(a)
Number of flashes with that spread
0
2
4
6
0
1
2
3
4
5
6
Vertical spread of pulse-pair heights, within single flash (km)

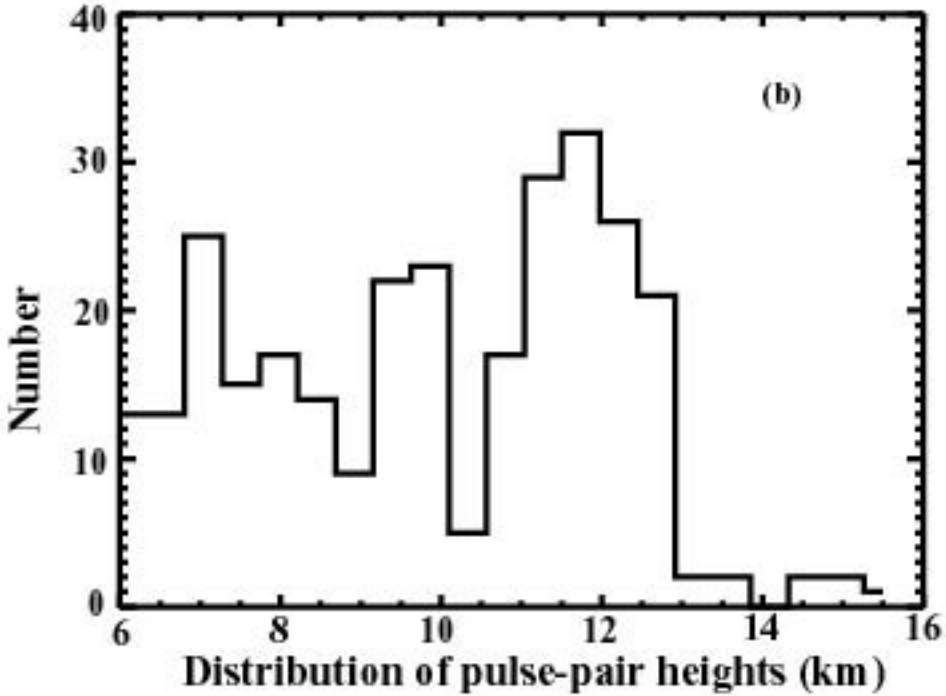
(b)
Number
0
10
20
30
40
6
8
10
12
14
16
Distribution of pulse-pair heights (km)

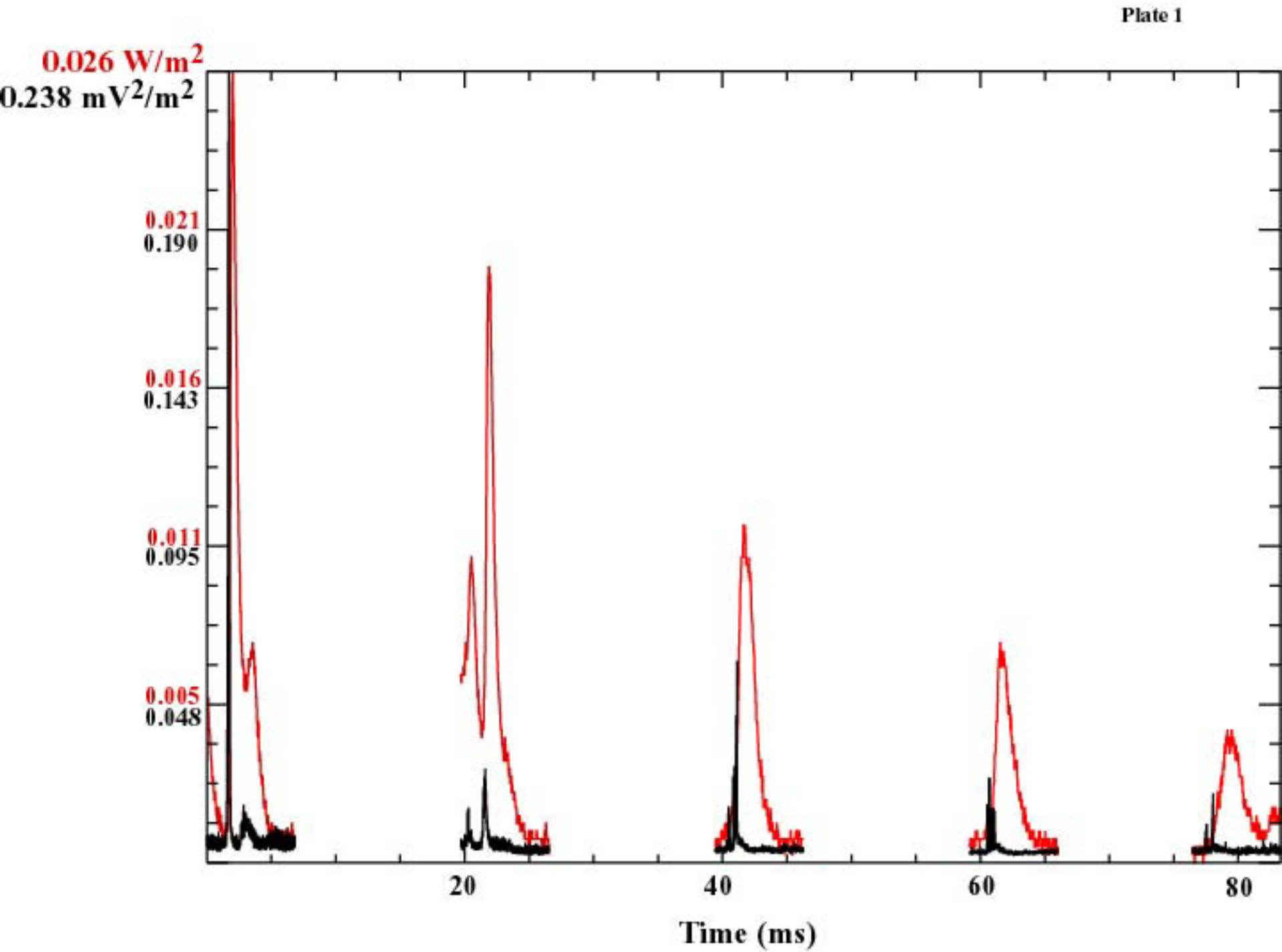
Plate 1
0.026 W/m2
0.238 mV2/m2
0.021
0.190
0.016
0.143
0.011
0.095
0.005
0.048
20
40
60
80
Time (ms)